Quasi-exactly solvable quartic: real algebraic spectral locus

Alexandre Eremenko and Andrei Gabrielov*

October 11, 2011

Abstract

We describe the real quasi-exactly solvable spectral locus of the PT-symmetric quartic using the Nevanlinna parametrization.
MSC: 81Q05, 34M60, 34A05.
Keywords: one-dimensional Schrödinger operators, quasi-exact solvability, PT-symmetry, singular perturbation.

Following Bender and Boettcher [3], we consider the eigenvalue problem in the complex plane

$$w'' + (\zeta^4 + 2b\zeta^2 + 2iJ\zeta + \lambda)w = 0, \quad w(te^{-\pi i/2 \pm \pi i/3}) \to 0, \quad t \to +\infty, \quad (1)$$

where J is a positive integer. This problem is quasi-exactly solvable [3]: there exist J elementary eigenfunctions $w = p_n(\zeta)\exp(-i\zeta^3/3 - ib\zeta)$, where p_n is a polynomial of degree $n = J - 1$.

When b is real, the problem is PT-symmetric. By the change of the independent variable $z = i\zeta$, (1) is equivalent to

$$-y'' + (z^4 - 2bz^2 + 2Jz)y = \lambda y, \quad y(te^{\pm \pi i/3}) \to 0, \quad t \to +\infty. \quad (2)$$

Polynomial h in the exponent of an elementary eigenfunction $y(z)$ is $h(z) = z^3/3 - bz$. The *spectral locus* Z_J is defined as

$$\{(b, \lambda) \in \mathbf{C}^2 : \exists\, y \neq 0 \text{ satisfying } (2)\}.$$

*Both authors are supported by NSF grant DMS-1067886.

The *real spectral locus* $Z_J(\mathbf{R})$ is $Z_J \cap \mathbf{R}^2$. The *quasi-exactly solvable spectral locus* Z_J^{QES} is the set of all $(b,\lambda) \in Z_J$ for which there exists an elementary solution y of (2). This is a smooth irreducible algebraic curve in $\mathbf{C}^2$, [1, 2]. In this paper we describe $Z_J^{QES}(\mathbf{R}) = Z_J^{QES} \cap \mathbf{R}^2$. We prove a result announced in [6]:

Theorem 1. For $n \geq 0$, $Z_{n+1}^{QES}(\mathbf{R})$ *consists of* $[n/2]+1$ *disjoint analytic curves* $\Gamma_{n,m}$, $0 \leq m \leq [n/2]$ *(analytic embeddings of* $\mathbf{R}$ *to* $\mathbf{R}^2$*).*

For $(b,\lambda) \in \Gamma_{n,m}$*, the eigenfunction has* n *zeros,* $n-2m$ *of them real.*

If n *is odd, then* $b \to +\infty$ *on both ends of each curve* $\Gamma_{n,m}$*. If* n *is even, then the same holds for* $m < n/2$*, but on the ends of* $\Gamma_{n,n/2}$ *we have* $b \to \pm\infty$*.*

If $(b,\lambda) \in \Gamma_{n,m}$, $(b,\mu) \in \Gamma_{n,m+1}$ *and* b *is sufficiently large, then* $\mu > \lambda$*.*

This theorem establishes the main features of $Z_{n+1}^{QES}(\mathbf{R})$ which can be seen in the computer-generated figure in [3]. Similar results were proved in [5] for two other PT-symmetric eigenvalue problems.

Our theorem parametrizes *all* polynomials P of degree 4 with the property that the differential equation $y''+Py=0$ has a solution with n zeros, $n-2m$ of them real [10, 7, 5].

Suppose that $(b,\lambda) \in Z_J^{QES}(\mathbf{R})$. Then the corresponding eigenfunction y of (2) can be always chosen real. Let y_1 be a real solution of the differential equation in (2) normalized by $y_1(x) \to 0$ as $x \to +\infty$, $x \in \mathbf{R}$. Then y_1 is linearly independent of y. Consider the meromorphic function $f = y/y_1$. This function has no critical points in $\mathbf{C}$, and the only singularities of f^{-1} are six logarithmic branch points. A meromorphic function in $\mathbf{C}$ with no critical points and whose inverse has finitely many logarithmic singularities is called a *Nevanlinna function*. All Nevanlinna functions f arise from differential equations $y''+Py=0$, where P is a polynomial by the above construction: f is a ratio of two linearly independent solutions of the differential equation.

Consider the sectors

$$S_j = \{te^{i\theta} : t>0,\ |\theta - \pi j/3| < \pi/6\}, \quad j=0,\dots,5.$$

The subscript j in S_j will be always understood as a residue modulo 6. Function f has asymptotic values $\infty, 0, c, 0, \overline{c}, 0$ in the sectors $S_0, \dots S_5$, where $c \in \overline{\mathbf{C}}$. It is known that f must have at least 3 distinct asymptotic values [9], so $c \neq 0, \infty$. Function f is defined up to multiplication by a non-zero real number, so we can always assume that $c = e^{i\beta}$, $0 \leq \beta \leq \pi$, where the points 0 and π can be identified. The asymptotic value c is called the *Nevanlinna*

parameter. There is a simple relation between c and the Stokes multipliers [11, 8].

The sectors S_j correspond to logarithmic singularities of the inverse function f^{-1}. Thus f^{-1} has 6 logarithmic singularities that lie over 4 points if $c \neq \overline{c}$, or over 3 points if $c = \overline{c}$.

The map $(b, \lambda) \mapsto \beta \pmod{\pi}$, $Z_J^{QES}(\mathbf{R}) \to \mathbf{R}$ is analytic and locally invertible [11, 2], so β can serve as a local parameter on the real QES spectral locus. To obtain a global parametrization one needs suitable charts on $Z_J^{QES}(\mathbf{R})$, where this map is injective.

To recover f, one has to know the asymptotic value c and one more piece of information, a certain cell decomposition of the plane described below. Once f is known, b and λ are found from the formula

$$\frac{f'''}{f'} - \frac{3}{2}\left(\frac{f''}{f'}\right)^2 = -2(z^4 - 2bz^2 + 2Jz - \lambda). \tag{3}$$

Now we describe, following [4], the cell decompositions needed to recover f from c. Suppose first that $c \notin \mathbf{R}$.

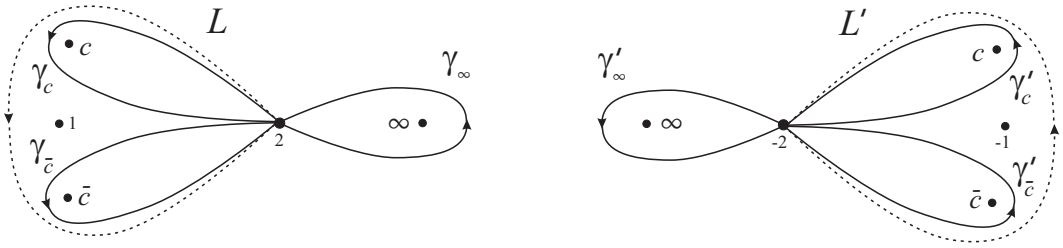

Fig. 1. Cell decompositions Φ and Φ' of the sphere (solid lines).

Consider the cell decomposition Φ of the Riemann sphere $\overline{\mathbf{C}}$ shown by solid lines in the left part of Fig. 1. It consists of one vertex at the point 2, three edges (loops γ_c, $\gamma_{\overline{c}}$ and γ_∞ around non-zero asymptotic values) and four faces (cells of dimension 2). The faces are labeled by the asymptotic values $0, c, \overline{c}, \infty$. Label 0 is not shown in the picture. The face labeled 0 is the unbounded region in the picture. (The point 1 in the figure is neither a label, nor a part of the cell decomposition. It will be needed, together with the dashed line L, for the limit at $\beta = 0$.) As

$$f : \mathbf{C} \setminus f^{-1}(\{0, \infty, c, \overline{c}\}) \to \overline{\mathbf{C}} \setminus \{0, \infty, c, \overline{c}\}$$

is a covering map, the cell decomposition Φ pulls back to a cell decomposition Ψ of the plane.

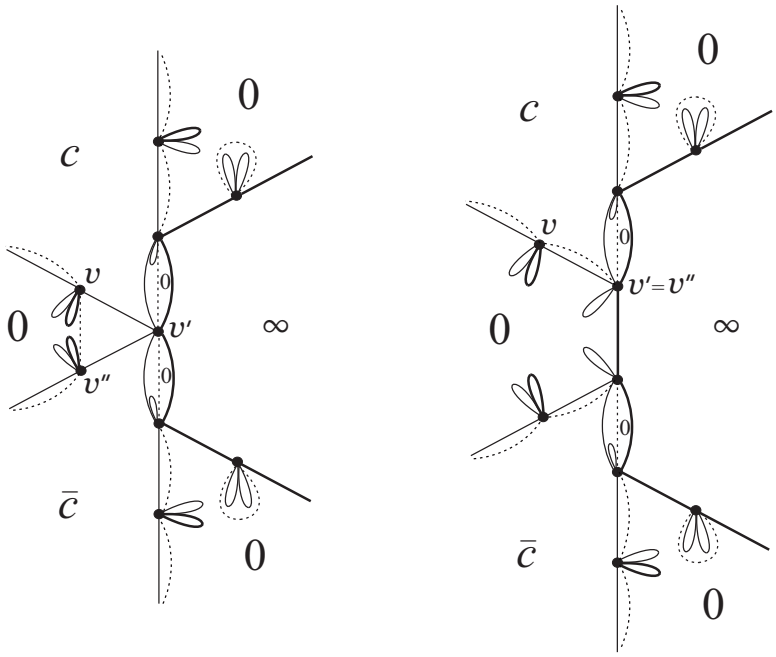

Fig. 2. Two examples of the cell decomposition Ψ of the plane (solid lines). Both eigenfunctions have two zeros, none of them real.

Examples of Ψ are shown with solid lines in Figs. 2 and 4 (left). The faces of Ψ are labeled with the same labels as their images. Non-zero labels of bounded faces are omitted in the picture. The reader can restore them from the condition that labels around a vertex must be in the same cyclic order as in Fig. 1 (left, solid lines). The labeled cell decomposition Ψ defines f up to a pre-composition with an affine map of $\mathbf{C}$. Two cell decompositions define the same f if they can be obtained from each other by a homeomorphism of the plane preserving orientation and the labels. Such cell decompositions are called equivalent.

By replacing multiple edges of the 1-skeleton of Ψ with single edges and removing the loops, we obtain a simpler cell decomposition T whose 1-skeleton is a tree, which we denote by the same letter T. The cell decomposition Ψ is uniquely recovered from its tree T embedded in the plane, [4]. The faces of T are asymptotic to the sectors S_j and the labels are the asymptotic values

in S_j. Two faces with a common edge cannot have the same label. The cell decomposition T is invariant under the reflection in the real axis, with simultaneous interchange of c and $\bar{c}$. It is easy to classify all possible embedded planar trees T with labeled faces that satisfy these properties. They depend on two integer parameters k and l with $l \geq 0$. These trees form two families, $\{X_{k,l},\ k \geq 0, l \geq 0\}$ and $\{X_{k,l},\ k < 0, l \geq 0\}$, shown in Fig. 3. Integers $|k|$ and l are the numbers of edges between ramification vertices, as shown in Fig. 3.

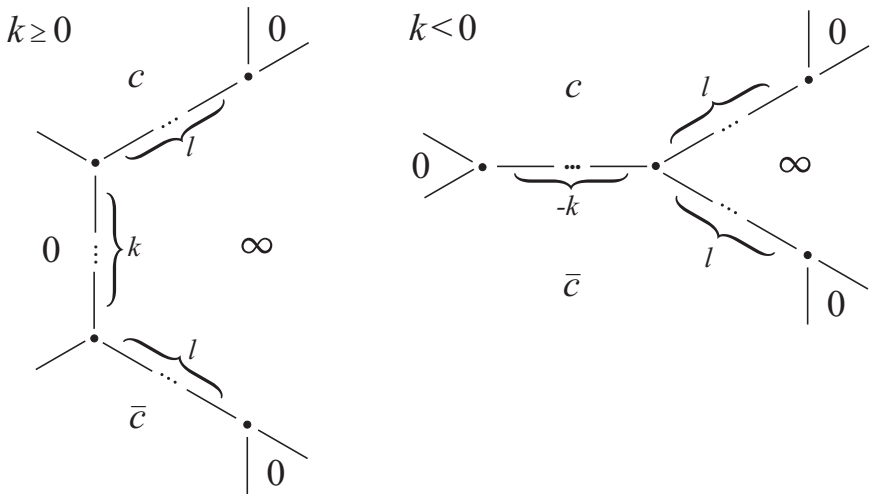

Fig. 3. Trees $X_{k,l}$.

Cell decompositions in Fig. 2 (solid lines) correspond to the trees $X_{0,1}$ and $X_{1,1}$. Cell decomposition in the left part of Fig. 4 (solid lines) corresponds to the tree $X_{-1,1}$ in the right part of Fig. 4.

Parameters of the trees $X_{k,l}$ can be interpreted as follows:

$$k^- := \min\{-k, 0\}$$

is the number of real zeros of f, and $2l$ is the number of non-real zeros. So the total number of zeros is $n = 2l + k^-$.

Functions f corresponding to the trees $X_{k,l},\ k \geq 0$, have $2l$ zeros, none of them real. Zeros of the eigenfunction y coincide with those of f.

For given n, the number of trees $X_{k,l}$ with $k < 0,\ 2l - k = n$ is

$$(n+1)/2 \text{ when } n \text{ is odd, and } n/2 \text{ when } n \text{ is even.} \tag{4}$$

Every tree $X_{k,l}$ and every $\beta \in (0,\pi)$ defines a meromorphic function f satisfying (3) with $J = 2l + k^- + 1$ and some (b,λ) depending on β, k and l. This follows from a result of Nevanlinna [9], see also [4]. From this function f, the coordinates of a point (b,λ) on the real QES spectral locus are recovered from the Schwarz equation (3). Thus we have a map $F : (T,\beta) \mapsto (b,\lambda)$ which we call the *Nevanlinna map.* This map is of highly transcendental nature: construction of f from T and β involves the uniformization theorem. We refer to [4, 5, 9] for details.

Each of the trees from our classification defines a chart of $Z_J^{QES}(\mathbf{R})$. To obtain the global parametrization of $Z_J^{QES}(\mathbf{R})$, we only have to find out how these charts are pasted together. We will see that the boundaries of our charts correspond to the values $c = \pm 1$.

Proof of Theorem 1. We begin with the charts $X_{k,l}$, $k < 0$. We show that in these charts the limits as $\beta \to 0$, π do not belong to the spectral locus. This is proved by the arguments similar to those in [5, Thm. 4.1].

Lemma 1. *For $k < 0$ and $l \geq 0$, the limit of the Nevanlinna map is*

$$\lim_{\beta \to 0} F(X_{k,l},\beta) = \infty.^1$$

Proof. When $\beta \to 0$, we have $c \to 1$, $\overline{c} \to 1$. Suppose by contradiction that $F(X_{k,l},\beta)$ has a limit (b_0,λ_0). Then there is a limit function f_0, a solution of the Schwarz equation (3) with these parameters b_0 and λ_0. Meromorphic function f_0 has three asymptotic values, $0, 1, \infty$, and we are going to find the corresponding cell decomposition. Let Φ_1 be the cell decomposition of the Riemann sphere with one vertex at the point 2 and two loops, γ_∞ and L (see Fig. 1, left). Let $\Psi_1 = f^{-1}(\Phi_1)$.

It is easy to construct Ψ_1 from the original cell decomposition Ψ. First, removing preimages of γ_c and $\gamma_{\overline{c}}$, we obtain the cell decomposition Ψ_∞, the preimage of the loop around ∞ in Φ. It is shown with the bold solid lines in Fig. 4.

Next, for each vertex v of Ψ consider the path L_v consisting of the edge of $f^{-1}(\gamma_c)$ starting at v and ending at some vertex v', followed by the edge of $f^{-1}(\gamma_{\overline{c}})$ starting at v' and ending at some vertex v''. Then the edge of $f^{-1}(L)$ from v to v'' is homotopic to L_v in the complement of Ψ_∞. The new edges

[1] Here ∞ refers to a point added to the (b,λ)-plane in the one-point compactification.

are shown with dashed lines in Fig. 4. The resulting cell decomposition is equivalent to Ψ_1.

Let V be the set of the vertices of Ψ contained in the boundary of the sector S_3. It is connected to the rest of the vertices of Ψ only at one vertex (v' in Fig. 4, left) which is also at the boundary of both sectors S_2 and S_4. The dashed line replacing the edges of Ψ that connect v' to the two adjacent vertices of V (v and v'' in Fig 4, left), goes from v to v''. All other dashed lines connect the vertices of $V \setminus \{v'\}$ with the other vertices from the same set. Hence $V \setminus \{v'\}$ is the set of vertices of a connected component of the 1-skeleton of the cell decomposition Ψ_1. This contradicts our assumption that $\Psi_1 = f_0^{-1}(\Phi_1)$, since the 1-skeleton of $f_0^{-1}(\Phi_1)$ must be connected. This contradiction proves the lemma.

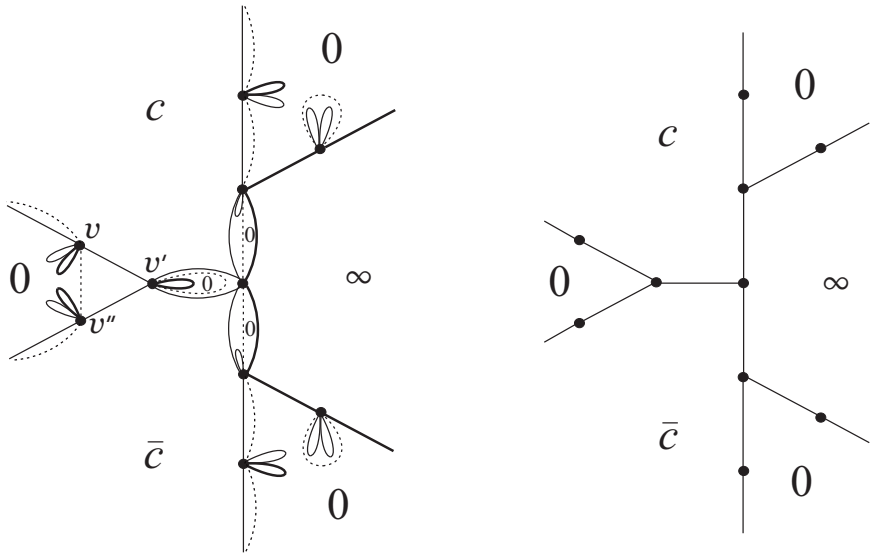

Fig. 4. A cell decomposition Ψ (solid lines) and the corresponding tree $X_{-1,1}$. Eigenfunction has one real and two non-real zeros.

Remark. Consider all meromorphic functions with no critical points and at most 6 asymptotic values. These functions f are defined by their asymptotic values and cell decompositions. Assume that one vertex v_0 of Ψ is placed at $z = 0$ and normalize so that $f'(0) = 1$. The class of normalized functions

obtained in this way is *compact* [12]. Let $f_\nu \to f_0$ be a converging sequence.[2] The 1-skeletons of the corresponding cell decompositions $\Psi(\nu)$ converge to the 1-skeleton of the cell decomposition $\Psi(0)$ as embedded graphs with a marked vertex. If two asymptotic values collide in the limit, one has to use the procedure described in the proof of Lemma 1: replacing two loops by one loop. The limiting cell decomposition obtained in Lemma 3 suggests that the eigenvalue problem (2) tends to a harmonic oscillator when $c \to 1$, the fact we'll later prove by different arguments.

Lemma 2. *For $k < 0$ and $l \geq 0$,*

$$\lim_{\beta \to \pi} F(X_{k,l}, \beta) = \infty.$$

Proof. When $\beta \to \pi$, we have $c \to -1$, $\bar{c} \to -1$. Suppose by contradiction that $F(X_{k,l}, \beta)$ has a limit (b_0, λ_0). Then there is a limit function f_0, a solution of the Schwarz equation (3) with these parameters b_0 and λ_0. Meromorphic function f_0 has three asymptotic values, $0, -1, \infty$, and we are going to find the corresponding cell decomposition.

To do this, it is convenient to choose another cell decomposition Φ' of the Riemann sphere, shown in the right part of Fig. 1 (solid lines). When $c \to -1$, Φ' collapses to Φ'_{-1} where the two loops γ'_c and $\gamma'_{\bar{c}}$ are replaced with a single loop L' around -1 (dashed line in Fig. 1, right).

We need the transition formula from $\Psi = f^{-1}(\Phi)$ to $\Psi' = f^{-1}(\Phi')$. This formula is obtained by combining the two decompositions (see Fig. 5) and expressing the loops of Φ' in terms of the loops of Φ.

[2] Uniform convergence on compact subsets in the plane, with respect to the spherical metric in the target sphere.

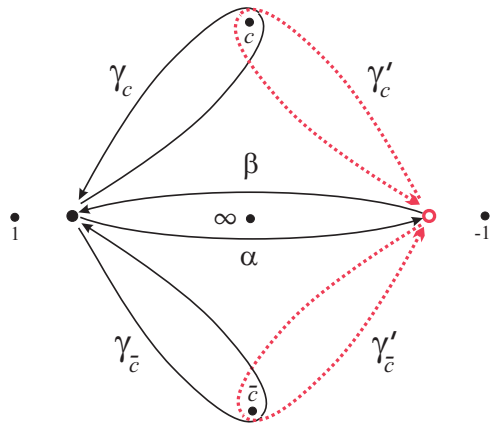

Fig. 5. Two cell decompositions of Fig. 1 combined.

The formulas, using notations in Fig. 5, are:

$$\gamma_\infty = \alpha\,\beta, \quad \gamma'_\infty = \beta\,\alpha, \quad \gamma'_c = \beta\,\gamma_c\,\beta^{-1}, \quad \gamma'_{\bar{c}} = \alpha^{-1}\,\gamma_{\bar{c}}\,\alpha. \tag{5}$$

Here the product should be read left to right. Similar formulas were obtained in [5] in the proof of Theorem 4.1. Application of these transition formulas to the cell decomposition Ψ of type $X_{-1,1}$ is illustrated in Figs. 6,7. In Fig. 6 the circles denote the vertices of Ψ' (preimages of the vertex of Φ') and the dotted lines correspond to the preimages of γ'_c and $\gamma'_{\bar{c}}$ determined from (5). The preimages of γ_∞ and γ'_∞ coincide. They are shown with the bold solid line.

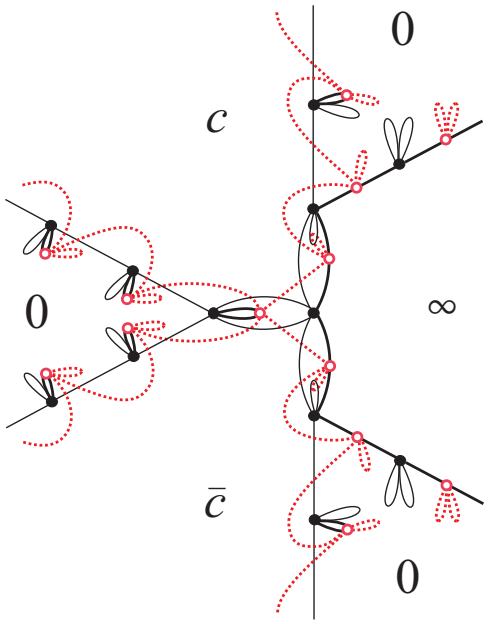

Fig. 6. Transition formulas (5) applied to the cell decomposition Ψ in Fig. 4.

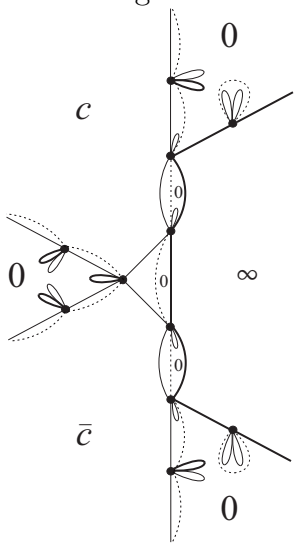

Fig. 7. Cell decomposition Ψ' (solid lines) corresponding to the cell decomposition Ψ in Fig. 4.

The same arguments as in Lemma 1 show that the 1-skeleton of the degener-

ation Ψ'_{-1} of Ψ' as $\beta \to \pi$ (shown with dotted lines in Fig. 7) is not connected. This proves the lemma.

Lemmas 1 and 2 show that for $k < 0$, the charts $X_{k,m}$ with $2m - k = n$ cover connected components of $Z^{QES}_{n+1}(\mathbf{R})$, each parametrized by $\beta \in (0, \pi)$. We call these components $\Gamma_{n,m}$. These are simple disjoint analytically embedded curves in $\mathbf{R}^2$.

When $\beta \to 0, \pi$ we must have $b \to \pm\infty$. We'll show below that $b \to +\infty$ on both ends of $\Gamma_{n,m}$ when $k < 0$.

When n is odd (that is J is even), these curves $\Gamma_{n,m}$ constitute the whole spectral locus $Z^{QES}_{n+1}(\mathbf{R})$.

Now consider the part of the spectral locus covered by the charts $X_{k,l},\ k \geq 0$. This part is present only when $n = 2l$ is even.

Lemma 3. *For $k \geq 0$ and $l \geq 0$, we have*

$$\lim_{\beta \to \pi} F(X_{k,l}, \beta) = \lim_{\beta \to 0} F(X_{k+1,l}, \beta). \tag{6}$$

and

$$\lim_{\beta \to 0} F(X_{0,l}, \beta) = \infty. \tag{7}$$

Proof of Lemma 3. This is similar to the arguments in Lemmas 1 and 2. Computation is illustrated in Figs. 2, 8, 9 and 10.

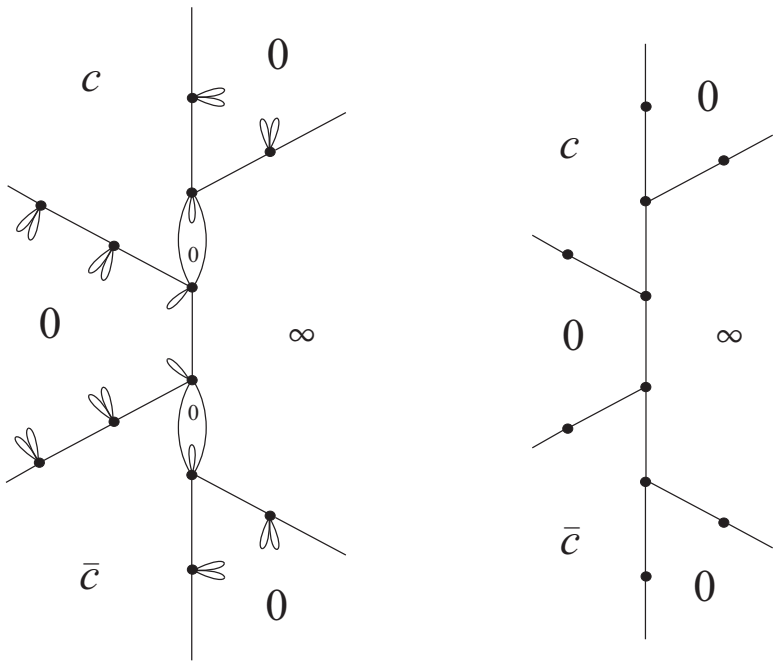

Fig. 8. Cell decomposition Ψ corresponding to $X_{1,1}$.

In the left part of Fig. 8 we use Ψ from Fig. 2, right. It corresponds to the tree $X_{1,1}$ in Fig. 8, right.

In Fig. 9 the circles denote the vertices of Ψ' (preimages of the vertex of Φ') and the dotted lines correspond to the preimages of γ'_c and $\gamma'_{\overline{c}}$ determined from (5). The preimages of γ_∞ and γ'_∞ coincide. They are shown with the bold solid line.

Removing the preimages of γ_c and $\gamma_{\overline{c}}$ (thin solid lines in Fig. 9) and the vertices of Ψ, we obtain the cell decomposition Ψ' shown in Fig. 10 (left) corresponding to the tree $X_{2,1}$ (right).

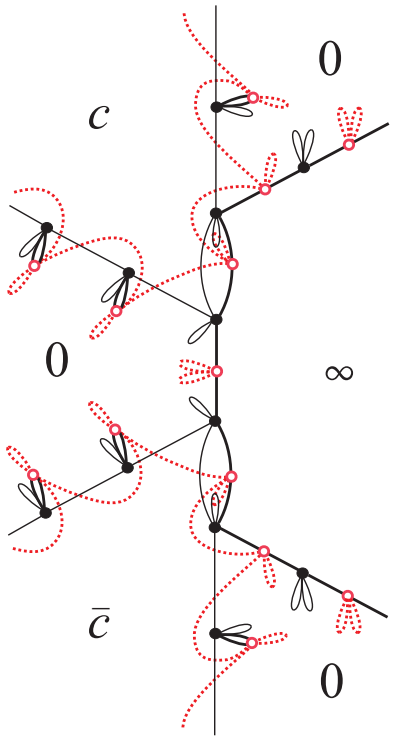

Fig. 9. Passing from Ψ to Ψ'.

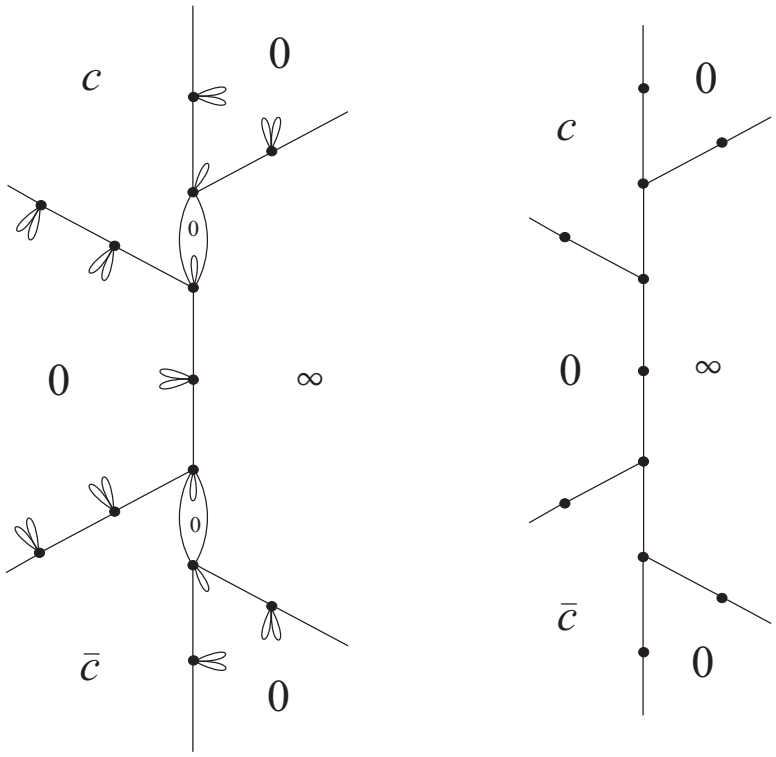

Fig. 10. Cell decomposition Ψ' corresponding to the tree $X_{2,1}$.

Thus, for $k \geq 0$, the cell decomposition Ψ'_{-1} of the plane obtained from $X_{k,l}$ in the limit $\beta \to \pi$ as the preimage of Φ'_{-1} is equivalent to the cell decomposition Ψ_1 obtained from $X_{k+1,l}$ in the limit $\beta \to 0$ as the preimage of Φ_1. Since $\Phi'_{-1} = -\Phi_1$, Nevanlinna theory implies that the corresponding functions f and f' satisfy $f' = -f$. (The symbol f' here should not be confused with the derivative.) Hence these two functions correspond to the same point of $Z_J^{QES}(\mathbf{R})$.

The proof of (7) is similar to that of Lemma 1. This completes the proof of the lemma.

Now we continue the proof of Theorem 1.

For even $n = 2l$, charts $X_{k,l},\ k \geq 0$ parametrize segments of one curve in the real QES spectral locus, and we call this curve $\Gamma_{n,n/2}$. We parametrize the curve $\Gamma_{n,n/2}$ by the real line, so that the number k decreases as the parameter t increases. Thus the chart $X_{0,n/2}$ corresponds to parameter values $t > t_0$. When the parameter t on $\Gamma_{n,n/2}$ tends to $+\infty$, the asymptotic value

$c = \exp(i\beta)$ tends to 1. On the other hand, when $t \to -\infty$ on $\Gamma_{n,n/2}$ the asymptotic value c does not have a limit; it oscillates, passing each point of the unit circle infinitely many times.

The curves $\Gamma_{n,m}$ are disjoint. Indeed, different cell decompositions give different functions f. This proves the first two statements of Theorem 1.

Now we deal with the asymptotic behavior of our curves $\Gamma_{n,m}$. We use the rescaling of (2) as in [6]. The QES spectral locus is defined by a polynomial equation $Q_{n+1}(b, \lambda) = 0$ which is of degree $n + 1$ in λ. So on a ray $b > b_0$ there are $n + 1$ branches $\lambda_j(b)$. In [6, Eq. (25)], we found that all λ_j have asymptotics $\lambda(b) \sim b^2 + O(\sqrt{b})$, $b \to \infty$, and as $b \to +\infty$, each QES eigenfunction y_j tends to some eigenfunction Y_ℓ of the harmonic oscillator

$$-Y'' + 4z^2 Y = \mu Y, \quad Y(it) \to 0, \quad t \to \pm\infty. \tag{8}$$

The eigenvalues of this harmonic oscillator are $\mu_\ell = 2(2\ell+1), \quad \ell = 0, 1, \dots$.

Only one of the eigenfunctions y_j can tend to a given Y_ℓ, and the corresponding eigenvalue satisfies

$$\lambda_j(b) = b^2 + (\mu_\ell - 2J + o(1))\sqrt{b}, \quad b \to +\infty.$$

It follows that all λ_j are real. The graph of each λ_j is a part of a curve $\Gamma_{n,m}$, and each $\Gamma_{n,m}$ has only two ends.

Now we consider the degeneration of the $X_{0,l}$ chart with $l \geq 0$, the chart which parametrizes the right end of $\Gamma_{n,n/2}$, $n = 2l$. On the end of $\Gamma_{n,n/2}$, where $t \to -\infty$ in the parametrization described after Lemma 3, there are infinitely many points $\Gamma_{n,n/2}(t_k)$ which belong to the real QES locus, and where the asymptotic value c is real. It was proved in [6] that these are exactly those points where $Z_J^{QES}(\mathbf{R})$ crosses the non-quasi-exactly solvable part of $Z_J(\mathbf{R})$, and these points correspond to $b_k \to -\infty$.

So only on one end of $\Gamma_{n,n/2}$ (where $t \to +\infty$) we can have $b \to +\infty$. On the other hand, each $\Gamma_{n,m}$, $m < n/2$ contains at most two graphs of λ_j. According to (4), the total number of these graphs λ_j is $n+1$, and the total number of curves $\Gamma_{n,m}$ is $(n + 1)/2$ when n is odd, and $n/2 + 1$ when n is even. It follows that, when n is odd, each $\Gamma_{n,m}$ contains two graphs of λ_j. When n is even, each $\Gamma_{n,m}$ except one contains two graphs of λ_j, while the exceptional component $\Gamma_{n,n/2}$ contains one graph of λ_j.

Thus $b \to +\infty$ as $c \to \pm 1$ in the $X_{k,l}$-charts with $k < 0$, which proves the third statement of Theorem 1. To prove the last statement, we study zeros of the eigenfunctions as $b \to +\infty$.

The eigenfunction Y_ℓ of (8) corresponding to the eigenvalue μ_ℓ has exactly ℓ zeros on $i\mathbf{R}$ and no other zeros in $\mathbf{C}$. One of these zeros is real iff ℓ is odd.

The trees corresponding to Y_ℓ are constructed similarly to those corresponding to y, using the two loop cell decomposition of the sphere, consisting of γ_∞ and the dashed loop in Fig. 1, left.

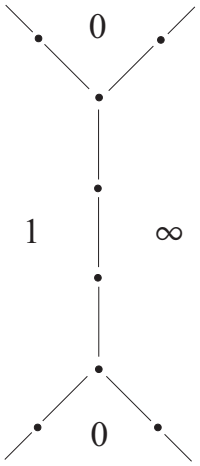

Fig. 11. The tree corresponding to Y_3.

For general results on convergence of Nevanlinna functions like our f we refer to [12].

When $b \to +\infty$, each QES eigenvalue $\lambda(b)$ must tend to some μ_ℓ, and the corresponding QES eigenfunction tends to Y_ℓ. Suppose that $\lambda(b) \in \Gamma_{n,m}$ with $m < n/2$. Then the tree corresponding to $\lambda(b)$ is $X_{k,m},\ k < 0,\ 2m - k = n$. From the arguments in the proofs of Lemmas 1 and 2 (see Figs. 4, 7), degeneration of the cell decomposition Ψ corresponding to such a tree has a connected component with $2m$ bounded faces when $\beta \to 0$ and with $2m + 1$ bounded faces when $\beta \to \pi$. This implies that the corresponding eigenfunction can only converge to Y_{2m} as $\beta \to 0$ and to Y_{2m+1} as $\beta \to \pi$.

If n is odd, these curves constitute the whole QES locus. If n is even, there is one more branch $\lambda(b)$ of the QES locus for large positive b, the right end of $\Gamma_{n,n/2}$ corresponding to the tree $X_{0,n/2}$. From the proof of Lemma 3 (see Fig. 2, left) degeneration of the cell decomposition Ψ corresponding to such a tree has a connected component with n bounded faces when $\beta \to 0$. This implies that the corresponding eigenfunction can only converge to Y_n.

So the ordering of the ends of the curves $\Gamma_{n,m}$ corresponds to the natural ordering of the first $n+1$ eigenvalues of the harmonic oscillator. This completes the proof.

References

[1] P. Alexandersson and A. Gabrielov, On eigenvalues of the Schrödinger operator with a complex-valued polynomial potential, arXiv:1011.5833.

[2] I. Bakken, A multiparameter eigenvalue problem in the complex plane, Amer. J. Math. 99 (1977), no. 5, 1015–1044.

[3] C. Bender and S. Boettcher, Quasi-exactly solvable quartic potential, J. Phys. A 31 (1998), no. 14, L273–L277.

[4] A. Eremenko and A. Gabrielov, Analytic continuation of eigenvalues of a quartic oscillator, Comm. Math. Phys. 287 (2009), no. 2, 431–457,

[5] A. Eremenko and A. Gabrielov, Singular perturbation of polynomial potentials in the complex domain with applications to PT-symmetric families, arXiv:1005.1696, to appear in Moscow Math. J.

[6] A. Eremenko and A. Gabrielov, Quasi-exactly solvable quartic: elementary integrals and asymptotics, J. Phys. A: Math. Theor. 44 (2011) 312001.

[7] A. Eremenko and A. Merenkov, Nevanlinna functions with real zeros, Illinois J. Math. 49 (2005) 1093–1110.

[8] D. Masoero, Y-System and Deformed Thermodynamic Bethe Ansatz, Lett. Math. Phys. 94 (2010), 151–164.

[9] R. Nevanlinna, Über Riemannsche Flächen mit endlich vielen Windungspunkten, Acta Math. 58 (1932) 295–373.

[10] K. Shin, All cubic and quartic polynomials P for which $f'' + P(z)f = 0$ has a solution with infinitely many real zeros and at most finitely many non-real zeros, Abstracts AMS 1057-34-26 (Lexington, KY, March 27-28, 2010).

[11] Y. Sibuya, Global theory of a second order linear ordinary differential equation with a polynomial coefficient, North Holland, Amsterdam, 1975.

[12] L. Volkovyski, Converging sequences of Riemann surfaces, Mat. Sbornik, 23 (65) N3 (1948) 361–382.

Department of Mathematics
Purdue University
West Lafayette, IN 47907
eremenko@math.purdue.edu
agabriel@math.purdue.edu